



TEOS Modified With Nano-Calcium Oxalate and PDMS to Protect Concrete Based Cultural Heritage Buildings

Kali Kapetanaki¹, Eleftheria Vazgiouraki¹, Dimitris Stefanakis¹, Afroditi Fotiou¹, George C. Anyfantis², Ines García-Lodeiro³, Maria T. Blanco-Varela³, Ioannis Arabatzis² and Pagona N. Maravelaki^{1*}

¹ Laboratory of Materials of Cultural Heritage and Modern Building, School of Architecture, Technical University of Crete, Chania, Greece, ² NanoPhos S.A., Technological and Science Park of Lavrio, Lávrío, Greece, ³ Consejo Superior de Investigaciones Científicas - Instituto de Ciencias de la Construcción Eduardo Torroja (IETCC), Madrid, Spain

OPEN ACCESS

Edited by:

Gabriel Maria Ingo,
Italian National Research Council, Italy

Reviewed by:

Maria Laura Santarelli,
Sapienza University of Rome, Italy
Emma Paola Angelini,
Politecnico di Torino, Italy

*Correspondence:

Pagona N. Maravelaki
pmaravelaki@isc.tuc.gr

Specialty section:

This article was submitted to
Colloidal Materials and Interfaces,
a section of the journal
Frontiers in Materials

Received: 25 October 2019

Accepted: 14 January 2020

Published: 07 February 2020

Citation:

Kapetanaki K, Vazgiouraki E, Stefanakis D, Fotiou A, Anyfantis GC, García-Lodeiro I, Blanco-Varela MT, Arabatzis I and Maravelaki PN (2020) TEOS Modified With Nano-Calcium Oxalate and PDMS to Protect Concrete Based Cultural Heritage Buildings. *Front. Mater.* 7:16. doi: 10.3389/fmats.2020.00016

Cultural Heritage constructions of twentieth century consist largely of mortar and concrete substrates. These concrete structures have suffered different types of decay processes. One of the most widely used consolidants is the Tetraethoxysilane (TEOS), which forms the basis of most existing commercial strengthening agents to protect porous building materials against deterioration. A novel, non-toxic strengthening and protective agent for mortar and concrete substrates was synthesized in a one-pot sol-gel procedure, incorporating in TEOS, Polydimethyl siloxane (PDMS), and nanoparticles of synthesized calcium oxalate (CaOx). PDMS provided hydrophobicity and reduced surface tension that causes cracks on the surface of produced xerogel. The synthesized nanocomposite both in sol and xerogel form was assessed with a variety of analytical techniques (FTIR, XRF, SEM, Optical Microscopy, Dynamic Light Scattering, Thermogravimetric analysis). The excellent physical properties of the produced colloidal solution of the nanocomposite, such as low viscosity and density, allow a penetration up to 2 cm from the surface in the treated cement mortars. This involved improvement of the mechanical and physical properties, such as the dynamic modulus of elasticity and increased water repellency. The treated cement mortars exhibited well-preserved aesthetic surface parameters and significant maintenance of the treatment. Furthermore, no harmful byproducts were identified indicating the nanocomposite compatibility to the siliceous and carbonate nature of the treated cement mortars.

Keywords: PDMS-TEOS-nano-calcium oxalate nanocomposite, concrete conservation, hydrophobic consolidant, compatible, cultural heritage conservation

INTRODUCTION

Cultural heritage constructions of twentieth century consist largely of mortar and concrete substrates. Due to the time and weathering conditions, these structures undergo different types of decay processes (Schutter, 2012). One common methodology proposed for preserving concrete heritage is the use of structural and surface treatments. Among the different types of treatments we can highlight the use of impregnation treatments, such as the consolidant Tetraethoxysilane

(TEOS) that enables the filling of micro-cracks generated by the decay processes (Pigino et al., 2012; Barberena-Fernández et al., 2015, 2018; Pan et al., 2017).

Silicon compounds such as TEOS are widely used in the field of consolidation and protection of modern constructions and heritage monuments. TEOS penetrated in traditional stone-based substrate, forming a SiO_2 gel which acts as a new cement matrix. However, in the case of concrete-based substrate, the mechanism of interaction is different. In a first stage, the hydrolysis of TEOS takes place to produce $\text{Si}(\text{OH})_4$ groups and ethanol. In a second stage, two competitive processes can take place; (i) $\text{Si}(\text{OH})_4$ can polymerized forming a SiO_2 gel and (ii) $\text{Si}(\text{OH})_4$ groups can interact with the Original Portland Cement (OPC) hydrated phases [such as $\text{Ca}(\text{OH})_2$] to produce C-S-H gel, which is the main responsible of the binding properties of concrete (Moropoulou et al., 2004; Sandrolini et al., 2012).

TEOS based products fulfill many requirements, including the long-term stability and strength under adverse conditions. Some additional favorable features of them are correlated to the lack of toxicity, the easy way to apply and their high degree of penetration into the target area due to their initial low viscosity (Verganelaki et al., 2015). The exploitation of the aforementioned characteristics of TEOS-based consolidants to the restoration of building damages, combined with their simple and low cost synthesis route, establish them extremely promising for an extensive and massive production.

Despite all these special characteristics of the TEOS-based consolidants, in practice, they still suffer from some remarkable drawbacks. In particular, cracks are developed during the sol-gel drying process due to the exerted capillary pressure by the gel network. Furthermore, the inefficient chemical bonding of the silica to the non-silicate substrates may cause inefficient performance of the treatment. Another drawback is related to the limited hydrophobicity of these materials, thus the water ingress at the substrate is not avoided and the building decay can progress (Maravelaki-Kalaitzaki et al., 2006; Scherer and Wheeler, 2009). Last but not least, the unavoidable biological impact considerably contributes to the degradation of the consolidants and their further inefficient action onto the building (Ruffolo and La Russa, 2019).

In order to overcome the above limitations and to develop a more effective consolidating material, a variety of chemical species (metals, molecules, and nanoparticles) have been utilized (Scherer and Wheeler, 2009; Pinho et al., 2013). Advanced methods involve the utilization of modified silanes, as well as the addition of surfactants, salts, natural, and synthetic polymers (Son et al., 2009; Illescas and Mosquera, 2012). In several cases, the results are encouraging and the cracks are eliminated, due to the reduced capillary pressure and surface tension. Despite the progress that has been made concerning the cracks elimination, the limited effectiveness of TEOS on carbonate substrates still remains a significant issue to deal with.

During the past, a series of compounds were tested in order to improve the consolidation. Although calcium alkoxides or nanolimes have been suggested for this purpose, their

limited stability toward atmospheric conditions, the tendency to agglomerate and the pure penetration depth in the substrates have prevented from wide range practical application (Baglioni et al., 2013; Rodriguez-Navarro et al., 2013).

Another challenging issue that has to be overcome is related to building decay caused by the water penetration into the substrate. In most of the cases, TEOS-based consolidants with alkyl siloxane water repellents commonly employed to prevent or reduce water ingress. The reduction of the surface energy of the consolidant has come to the foreground as a critical parameter which can regulate the water repellency (Illescas and Mosquera, 2012; Karapanagiotis et al., 2014). An ordinary methodology includes the utilization of a consolidant with a hydrophobic coating or the incorporation of hydrophobic agents into the consolidant materials. In particular, a mixture of modified TEOS, PDMS, and n-octylamine has been referred as a satisfactory solution for the problem of the water wetting (Mosquera et al., 2010).

Calcium oxalate (CaC_2O_4) is the main component of patina, which is found on well-preserved monumental surfaces and historical buildings. Patina layers originating from biological agents or transformation of previous protective treatments, offered a protective role on monuments and building stones (Ion et al., 2017). The contribution of calcium oxalate (CaOx) is important to the surface protection of monuments, by forming a thin compact non-porous shell. The film is highly resistant to acid attack, due to its pH independence which is a determinant factor during the carbonation process.

In a previous work, an inorganic nanocomposite based on silica and calcium oxalate was proposed. More specifically, amorphous CaOx was incorporated into the silica matrix. The addition of CaOx to the TEOS increased the pore volume during the gel formation producing a crack-free xerogel. At the same time compatibility and affinity between the nanocomposite and substrate was achieved, as CaOx enabled electrostatic interactions, offering chemical affinity between the silica and the carbonaceous substrates (Verganelaki et al., 2014).

In this study, an improved modified one-pot synthesis of this silica nanocomposite enriched with CaOx, in order to dispose chemical affinity with the concrete based-substrates eliminating the cracks, is described. The innovation of this preparation involves the synthesis of CaOx during the polymerization of TEOS, as well as the addition of a hydrophobic agent, PDMS (hydroxyl-terminated polydimethylsiloxane). PDMS is an organosilane, which provides hydrophobicity and water repellency. The chemically bonded chains of PDMS induce discontinuities in the resulting network, contributing to increased deformability and porosity. Finally, the enhancement of toughness and flexibility of the silica network, prevent the gel from cracking during drying.

This novel treatment is tested on different types of OPC based-substrates (sound, chemically, and physically aged mortars) in order to check its effectiveness. Treatment uptake and penetration depth, as well as the changes in the mechanical, hydric, and color properties of the substrate have been evaluated after treatment.

EXPERIMENTAL PART

Materials

Tetraethyl orthosilicate (Tetraethoxysilane, TEOS), the hydroxyl-terminated polydimethylsiloxane (PDMS: MEM 0347), oxalic acid dihydrate (Ox), and calcium hydroxide (CH) were purchased from NanoPhos (NanoPhos S.A. Technological and Science Park, Lavrio, Greece). Isopropanol (ISP, Aldrich) and deionized water were used as solvents. All chemicals were used as received, without further purification prior to use. Additionally, a high molecular weight with polystyrene blocks copolymer, the commercial dispersant (Disperbyk-190, BYK-Chemie, Wesel) was added during the sol production, thus contributing to the reduction of the surface tension and the elimination of the cracking of xerogel.

Synthesis Route

The synthesis of the consolidant product, named as FX-C is presented in **Figure 1**. CaOx was formed at the first solution (designated A₁), which contained CH, water and Ox. The solution A₁ underwent magnetic stirring for 5 min. In a second step, a part of TEOS and ISP were added to the solution A₁ (solution A₂) and remained under magnetic stirring and ultrasonic agitation for 5 and 10 min, respectively. This is the first part of TEOS hydrolysis which is enforced by the presence of the Ox, which acts as a catalyst (Verganelaki et al., 2015). Simultaneously, another solution designated as sol B was prepared mixing PDMS, TEOS, and ISP and stirring for 10 min. Solutions A₂ and B were mixed and left under stirring for 7 h. The quantities were optimized after several experiments aimed at producing a colloidal solution with low viscosity (~2–3 mPa·s) and a crack free xerogel. The final molar ratio of the precursors and solvents TEOS/ISP/H₂O/Ox/CH was equal to 1/10.4/8.01/0.06/0.007.

Hydrolysis and condensation of TEOS were monitored through FTIR. The derived final solution was cast into cylindrical

transparent glass vessels of Ø35 × 38 mm dimensions. The vessels were appropriately covered in order to simulate the evaporation of solvent occurring into the pores of the cement substrate. The casting sols were exposed to laboratory conditions (RH = 60 ± 5%, T = 20 ± 2°C).

Test Methods

The produced nanocomposite was assessed with a variety of analytical techniques described in the following. A Brookfield DV-II + Pro spindle: S18 viscometer was used for the viscosity measurements of the sol vs. time with temperature control at 25°C. The percent volume and mass reduction of the xerogel was calculated from the volume and weight losses of the initial sol casted in the glass vessel. In order to get a first approximation concerning the surface tension of the solution, a pendant drop tensiometer was used according to EN Standard Procedure 15802:2009 (Berry et al., 2015). The FX-C xerogel was microscopically assessed with the aid of the digital microscope USB Dino-Lite AM4515T5 Edge. The microscope was equipped with a color CMOS sensor. The captured via the Dino Capture 2.0 software images had 1.3 megapixels resolution, and 500× zoom. The tests of Vickers hardness for the FX-C nanocomposite were performed with a microhardness tester Future-Tech FM-700, under loading of 300 g with dwell time 5 s. An optical tensiometer (Thetalite TL 101, KSV) was used for the contact angle measurements vs. time, determining the static contact angle (θ_s) of the FX-C itself.

A satisfactory insight into the evolution of the sol-gel process and the stability of the bonds between the newly formed chemical species was obtained via the Fourier transform infrared spectroscopy (FTIR) absorption spectra. The spectra were recorded with a PerkinElmer 1000 spectrometer, in the spectral range from 4,000 to 400 cm⁻¹.

The thermal behavior of the developed xerogel was carried out by thermogravimetric analysis (DTA-TG) in a Setaram LabSys

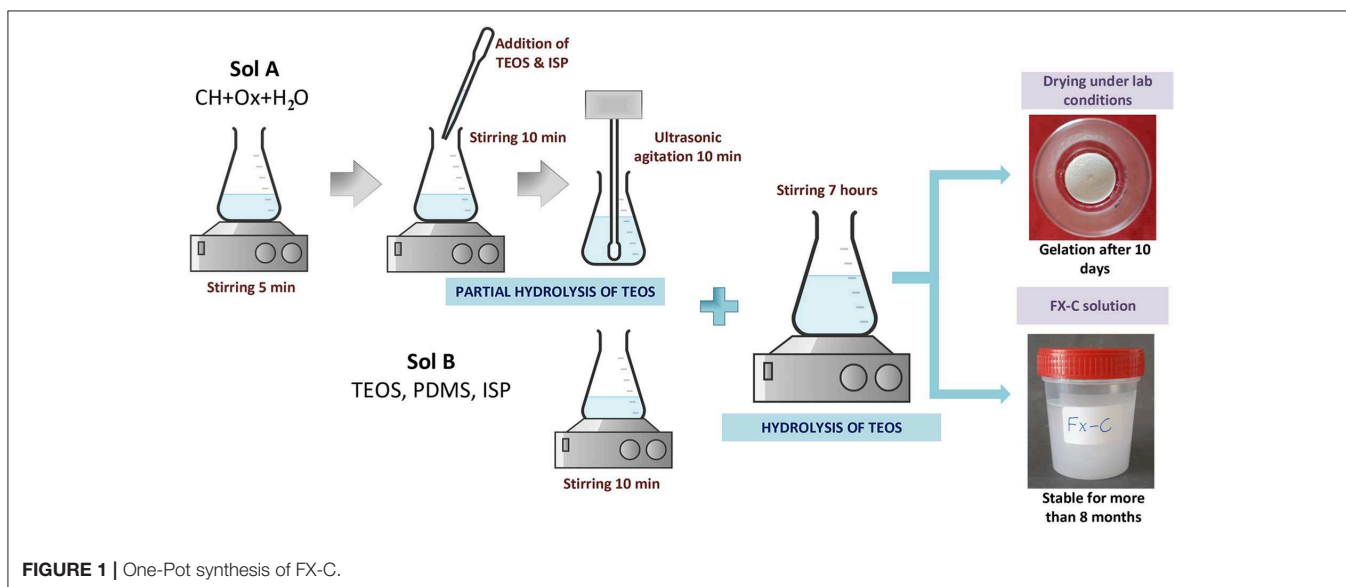


TABLE 1 | Properties of the colloidal solution and xerogel FX-C.

Sample	Viscosity (mPa·s)	Volume reduction (%v/v)	Weight reduction (%w/w)	pH	Density (gr/cm ³)	Gelation time (days)*	Sol appearance	Xerogel state	Hardness
Solution	2.05	–	–	2.93	0.85	10	White, one phase	–	–
Xerogel	–	71	49	–	–	–	White	Hard monolithic	199.3 Vickers

Evo 1,600°C. The sample under investigation was heated up to 1,000°C under nitrogen atmosphere with a heating rate of 10°C/min.

Scanning and transmission electron microscopy techniques (SEM and TEM, respectively) were used for the xerogel microstructure characterization. SEM micrographs were captured at the backscattered electrons mode using an energy-dispersive X-ray analysis system attached to a scanning electron microscope (Philips SEM 535 with EDAX equipment). Transmission electron microscopy (TEM) micrographs were recorded with a JEOL JEM 100C electron microscope operating at 200 kV, equipped with a Model 782 ES500W Erlangshen CCD camera.

Energy dispersive X-ray fluorescence (EDXRF) is a suitable technique for identifying the elemental composition of the compounds present at the xerogel. Measurements were directly performed on the xerogel sample ground to a powder. The EDXRF instrumentation included ¹⁰⁹Cd and ⁵⁵Fe radioactive sources, Si(Li) semiconductor detector (resolution 150 eV at 5.9 keV), TC-244 Spectroscopy Amplifier, PCA-II Nucleus Multichannel Card, AXIL (RN) computer program analysis.

A multimode AFM (Digital Instrumens Nanoscope IIIa) was used to study the AFM face images.

Total porosity and the average pore size diameter were determined by mercury intrusion porosimetry (MIP). Measurements were performed using Micrometrics Poresizer 9320. Aesthetic parameters (colorimetric analysis) were determined using a MINOLTA CM-2500d spectrophotometer.

Preparation of OPC Mortar Samples

OPC mortar specimens (with different sizes were prepared as specified in European standard EN 196-1 using CEM I 42.5R cement (Table S1), CEN-compliant sand at a cement/ratio of 1/3 and a water/cement ratio of 0.5 (sound mortars). Although no demolding product was applied, the inner surface of the mold was coated with a self-adhesive film. In order to simulate similar features than in an actual ordinary concrete, several sets of non-standard mortars were elaborated. Additionally, OPC non-standard mortars were prepared using a sand/cement ratio of 5/1 and water/cement ratio of 0.5.

The porosity of the non-standard mortars seemed to be closer to that of the deteriorated concrete surface, so they were selected to simulate the penetration way of the consolidant into the target substrate. To simulate the common types of decay processes in concrete, standard mortars were physically and chemically aged using different types of deterioration accelerated test. The aged

samples were selected in order to simulate the more characteristic types of concrete decay. For this reason, the aging processes that were followed were (1) aging by chemical degradation caused by (a) carbonation and (b) chloride penetration and (2) aging through physical degradation caused by freeze-thaw cycles.

Aging through carbonation took place by exposing OPC mortar samples in CO₂ incubator chamber (2% CO₂, 25°C, R.H > 80%) for 8 months. Sound specimens were subjected to 4 cycles of chloride penetration. Each cycle included the samples immersion in saturated solution of NaCl for 48 h, followed by drying at 105°C for 24 h. After the end of the aforementioned 4 cycles, the samples were immersed in deionized water, where they remained for 2 weeks. Concerning the aging process through the freeze-thaw cycles, each cycle of this procedure included two stages-processes: temperature reduction from 4 ± 2°C to –18 ± 2°C during half an hour and maintenance at the final temperature for 2.5 h (freeze process) and vice versa (thaw process). During the freeze stage the samples remained under air conditions while they were immersed into the water during the thaw cycle (AST C666). Samples were subjected to 28 repetitive cycles.

Once the aging process finishes, OPC mortars were characterized (Total porosity and average pore size diameter, colorimetric analysis, FTIR) by different techniques mentioned in sections Test Methods and FX-C Application on Cement Mortars Samples.

FX-C Application on Cement Mortars Samples

Three cubic specimens (50 × 50 × 50 mm) from each aging set were brushed only on one side. Before the FX-C application, the sample surface was gently polished with an abrasive paper of fine grit size (P180 carborundum paper). Next, the specimens were rinsed with deionized water. Their dry took place in an oven at 60 ± 2°C for 3 days. They weighed up to obtain a constant mass and then they remained in a desiccator vessel until the consolidant application. The samples were sprayed with ISP at the beginning and in the middle of the application process to facilitate the sol entrance and migration inside the pores of the substrate. The brushing of the sample with the consolidant have taken place uniformly in two directions (vertically and horizontally) in order to avoid the formation of a thick nanocomposite layer onto it with the subsequent formation of cracks at the surface. After treatment, samples were exposed to lab conditions, at RH = 60 ± 5% and T = 20 ± 2°C.

Tests Methods for the Evaluation of the Treatment

The performance of the developed consolidant was assessed using the techniques described below, at sound, aged (chemical or physical degradation) and non-standard samples treated with FX-C. Aging process is used in order to simulate the decay process of cement and concrete surfaces.

Aesthetic, physico-chemical, mechanical properties, microstructure, and composition of the samples were checked through tests of colorimetry, optical microscopy, contact angle, FTIR analysis, water capillarity, peeling test, ultrasound pulse velocity, and SEM.

The treatment of samples aimed to enhance physical and mechanical properties without altering aesthetic parameters, as well as without over-strengthening the substrate. The color modifications were studied using a Konica Minolta, CM-2600d and Vis spectrophotometer adapted with a D65 illuminant at 8-degree viewing, in a wavelength range from 360 to 740 nm. The average values of the color parameters L^* , a^* , and b^* , were derived from five measurements of random areas of untreated and treated specimens and used for the calculation of the total color difference expressed as ΔE^* (Maravelaki et al., 2014; Lollino et al., 2015).

Optical microscopy was used to monitor the treated surface 1 day after the application, in order the crack formation to be checked. The images were captured with the Dino Lite microscope (for more details concerning the specifications of the system see nanocomposite section).

In order to evaluate the hydrophobicity of surfaces, water contact angle (WCA) measurements were carried out using the tensiometer, as it has already been described at the nanocomposite test methods section. Measurements were in accordance to EN Standard Procedure 15802:2009. On different points of each specimen, several water droplets ($\sim 5 \mu\text{L}$) were deposited close to the surfaces using a needle. Afterwards, the images of the droplets were further processed revealing the average CA values. Additionally, water absorption by capillarity according to the EN 15801:2010 was performed to evaluate water repellency of treated samples (UNI 11432: 2011). The maximum water absorption per unit area (Q_i , expressed in $\text{mg}\cdot\text{cm}^{-1}$) and the capillary water absorption coefficients (CA) in $\text{mg}\cdot\text{cm}^{-1}\cdot\text{s}^{1/2}$ were calculated before and after treatment, for all the substrates. The amount of water absorbed by the specimen per unit area Q_i (kg/m^2) at time t_i (s) is calculated by the following equation:

$$Q_i = \frac{m_i - m_0}{A}$$

where, m_i is mass of the specimen at time t_i , in kg; m_0 is the mass of the dry specimen, in kg and A is the area of the specimen in contact with water, in m^2 . Additionally, water absorption coefficient by capillary (WCA) was estimated by the slope of linear section of the Q_i - $\sqrt{t_i}$ curve.

One of the most important parameters for evaluating the effectiveness of the consolidation is the determination of the penetration depth of the applied consolidant. The penetration

depth of the FX-C into the treated samples was evaluated with FTIR analyses. Powders derived from the surface and at different depths from sections of the treated samples under investigation, were analyzed by FTIR analysis. The evaluation of the FX-C penetration depth was based on the identification of the characteristic peaks of the Si-O-Si stretching at the FTIR spectra corresponding to the nanocomposite. Furthermore, the colloidal FX-C solution was stained with thymol blue and the penetration depth was visually inspected after cutting the specimen and measuring the stained sol penetration depth at the perpendicular sections.

Mechanical assessment was held by measuring Ultrasound Pulse Velocity (UPV). The dynamic modulus of elasticity (E_{dyn}) according to EN 14579 (2004), was calculated through the equation:

$$E_{\text{dyn}} = d \times V^2$$

where, d is the density of the sample and V the measured velocity of ultrasound pulse (Miliani et al., 2007). The density of the samples derived from the ratio of weight to volume; the latter, was calculated from the dimensions of samples.

Finally, the treatment-substrate interface of the treated samples with FX-C was visualized by SEM microscopy. Transversal sections of treated materials, and their untreated counterpart, coated with a thin conducting layer of gold, were examined.

RESULTS AND DISCUSSION

Characterization of the Consolidant FX-C

The prepared nanocomposite exhibits a Newtonian behavior at the shear range evaluated, with the viscosity to be calculated $2 \text{ mPa}\cdot\text{s}$, close to that of the commercial products. This value of viscosity indicates a sufficient and uniform penetration into the pores of inorganic materials, as the depth of penetration is related to the viscosity of the consolidants (Franzoni et al., 2014). Viscosity over time has been used as indicator of the consolidant stability. In this study, the viscosity remained unchanged under no evaporation conditions, according to the rheological observations.

The macroscopic evolution of the FX-C to gel, has been monitored by measuring the dry volume reduction. An amount of 71% was lost, which is comparable with similar xerogels referred in the literature (Facio et al., 2017). The derived xerogel has exhibited 70% weight loss (Table 1).

The macroscopic appearance of FX-C reveals a homogeneous monolithic xerogel, with a significant degree of cohesion and lack of crack. The surface tension of the FX-C sol was determined to be equal to $30 \pm 2 \text{ mN}/\text{m}$.

The FTIR spectra of the FX-C are illustrated in Figure 2. They reveal the effective co-polymerization of PDMS with TEOS, as well as the successful synthesis and incorporation of CaOx in the silica network.

In Figure 2, the FTIR spectrum (A) of solution A1 shows that CaOx was formed after the reaction of CH and Ox. In

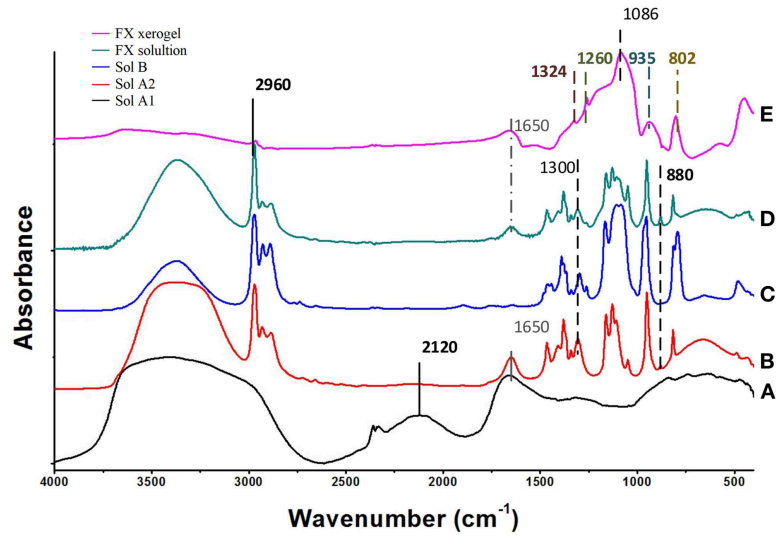


FIGURE 2 | FTIR spectra of the initial sols: (A) A1 (CH + H₂O + Ox), (B) A2 (ISP+TEOS) mixed with A1, (C) (TEOS+PDMS+ISP), (D) the derived FX-sol, and (E) the xerogel FX-C.

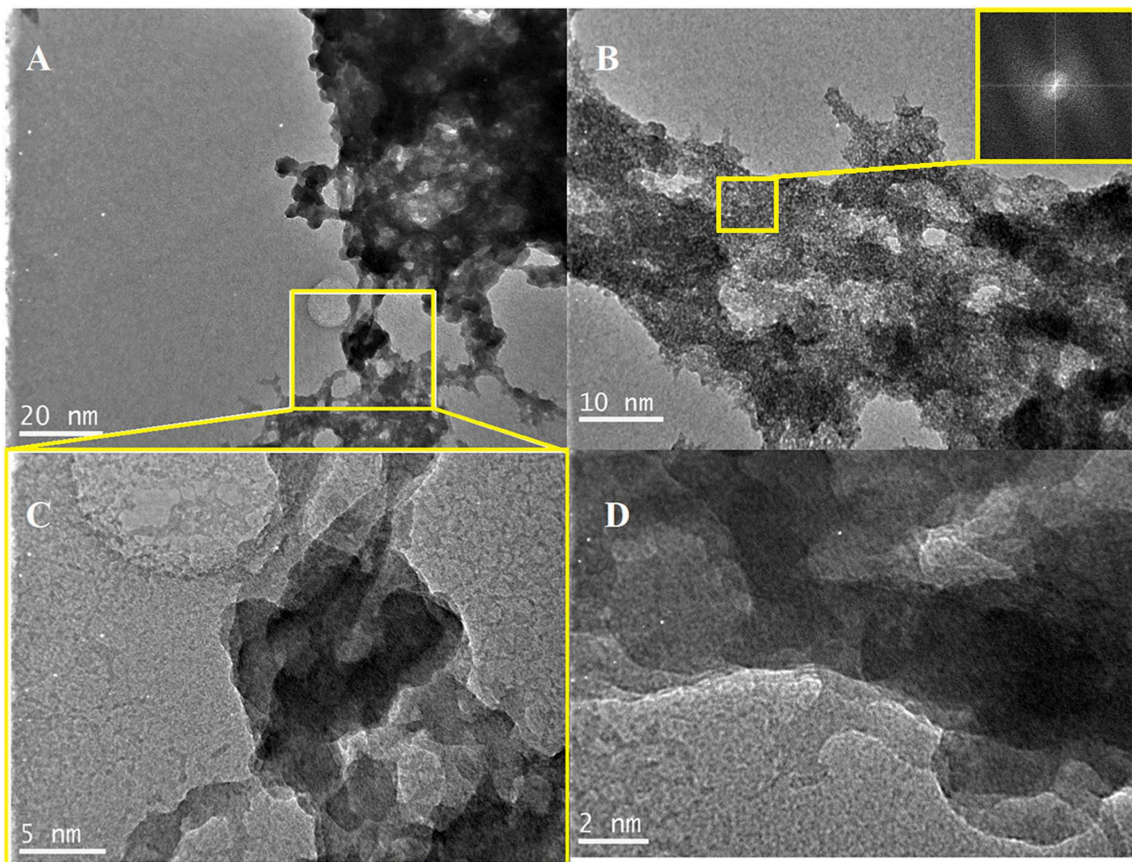
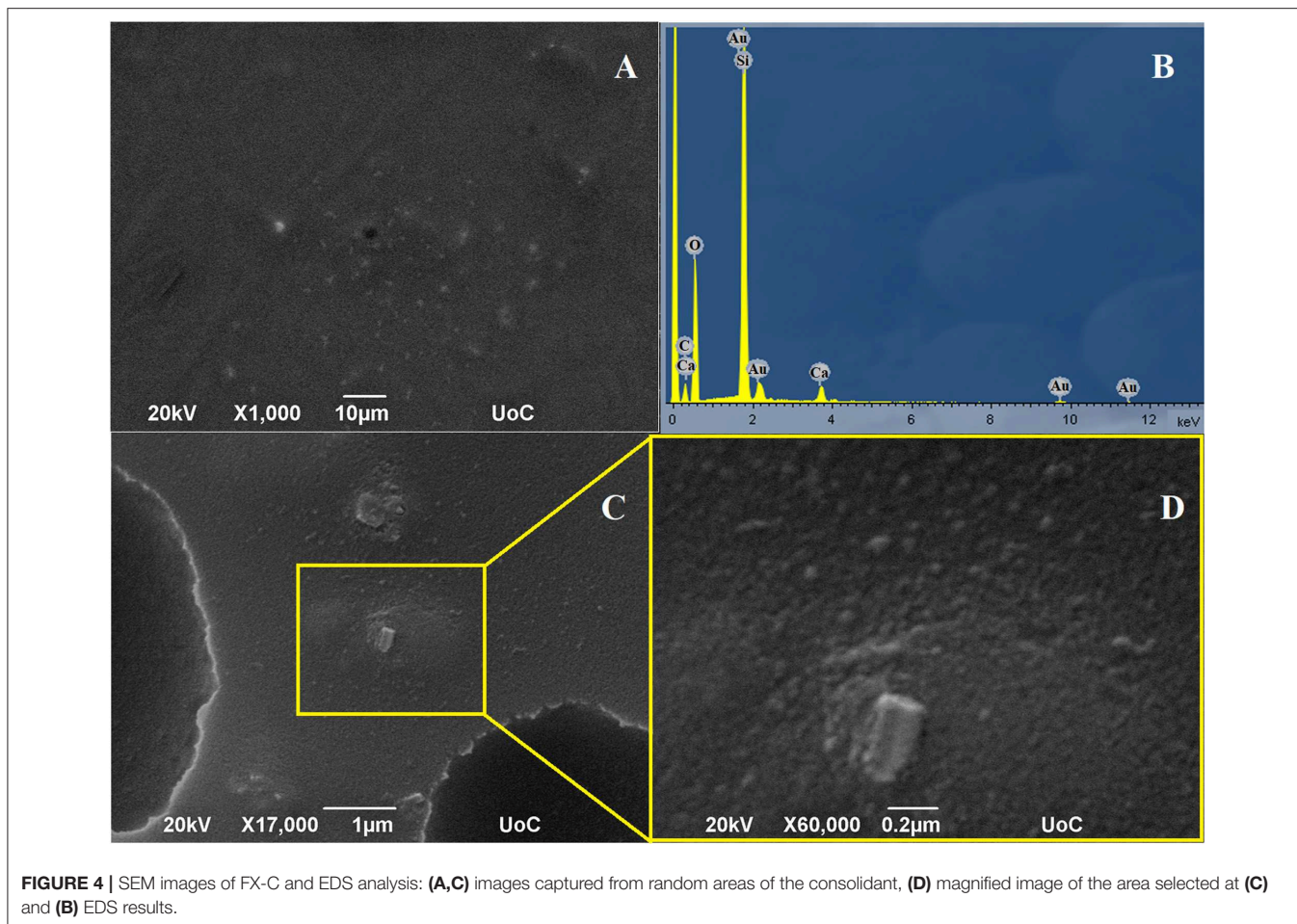
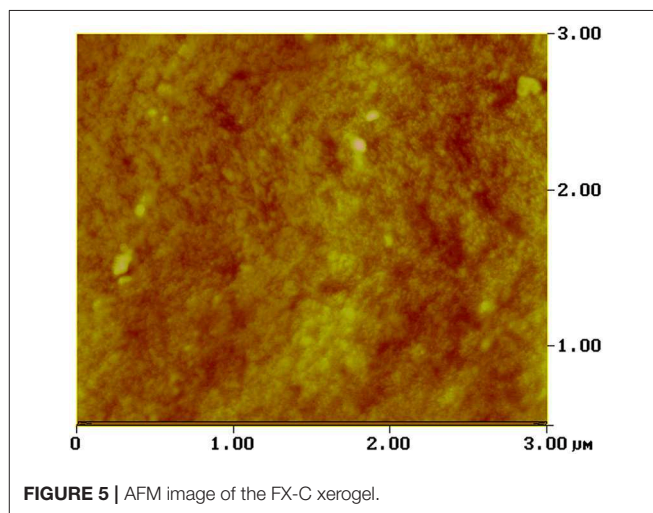


FIGURE 3 | TEM images of the produced consolidant: (A,B,D) images captured from random areas of the consolidant surface, (C) magnified image of the area selected at (A).



particular, the bands identified at $1,324$ and partially at $1,650\text{ cm}^{-1}$, are associated with the O-C-O symmetric and anti-symmetric stretching of CaOx, respectively (Maravelaki et al., 2014; Lin et al., 2019). The band located at $1,650\text{ cm}^{-1}$ overlaps with the absorbed water bending vibration. The stretching bands of CaOx are shown both in spectra of FX solution (E) and xerogel (D). In addition, the absence of the characteristic and very sharp absorption band of portlandite [CH: $\text{Ca}(\text{OH})_2$] at $3,640\text{ cm}^{-1}$ (spectrum A), indicates a consumption of CH, attributed to calcium isopropoxide transformation and reaction with Ox to yield CaOx (Verganelaki et al., 2015).

In the FTIR spectrum (B) of solution A2, a small band at 880 cm^{-1} is assigned to EtOH, which is produced from the hydrolysis of TEOS. After the mixing of A1 and A2 sols, FTIR bands of PDMS are observed at $2,960$, $1,260$, and 800 cm^{-1} . These bands correspond to antisymmetric stretching C-H bond in CH_3 , the symmetric bending of the CH_3 groups in Si-(CH_3) and rocking $-\text{CH}_3$ of PDMS molecules, respectively (spectrum C) (Kapridaki and Maravelaki-Kalaitzaki, 2013). The same bands are shown in FTIR of FX xerogel and FX sol (E, D), indicating the existence of PDMS to the final product. In addition, two strong infrared bands are present at $1,086$ and 802 cm^{-1} , which are assigned to the Si-O-Si antisymmetric and symmetric stretching vibrations, respectively. The FTIR spectrum of FX solution is



more complicated, due to the overlapping of ISP, TEOS, and ethanol bands.

FTIR spectra indicate the acid catalysis of TEOS by Ox. Indeed, the role of Ox is dual; firstly to allow the catalysis of TEOS and secondly to react with CH and to produce CaOx. The

silica network is determined by the Si-O-Si formation at 1,086 and 802 cm^{-1} , attributed to the antisymmetric and symmetric stretching of Si-O-Si groups, respectively. Furthermore, the band at 935 cm^{-1} is assigned to overlapping of the newly-formed Si-O-Si bonds between Si-OH groups of hydrolyzed TEOS, the unpolymerized parts of the silica matrix and the silanol groups of PDMS.

The morphological profile of FX-C was inspected by transmission electron microscopy (Figure 3). TEM images exhibit FX-C nanocomposite to be present in an aggregated form, finding that can be explained by the polymeric chain modification due to the CaOx and PDMS incorporation from electrostatic interaction and hydrogen bonding. TEM images displayed two phases; the first covered a large area of the FX-C consisted of amorphous SiO_2 , whereas the second one involved a semi-crystalline structure of the nanocomposite in the nanoscale. The semi-crystallinity of FX-C was confirmed by the characteristic pattern evidenced at the images captured with high magnification (Figure 3B). In addition, small dots are exhibited that are darker than the surrounding ones, as it is displayed in the images with the higher magnification. This appearance could be attributed to the nucleation seeds or crystal-like seeds. Another characteristic is the existence of dark and bright areas that could be attributed to different thickness produced by the PDMS and Ca^{2+} modification of the matrix.

Figure 4 shows the SEM micrographs of FX-C xerogel. A crack-free and roughed surface is displayed in the SEM images. The absence of cracking and micro-cracking is significant.

Different magnifications were received to inspect the surface morphology. The surface appeared to be considerably rough, as bumps and cavities were observed, due to TEOS and PDMS copolymerization process. The microstructure presented in Figure 4C which is presented with high magnification in Figure 4D, was identified as mainly silicon based, by EDS (Figure 4B). However, in other areas, as those indicated in the rectangular, Ca was also identified attributed to CaOx incorporated in the silica matrix. The elemental composition by EDS measurements (Figure 4B) confirmed the existence of calcium and silicon elements, related to CaOx and polymerized TEOS-PDMS, respectively. The appearance of the characteristic peaks of gold is due to the sputtering process, as this element was used to create a conductive layer. The results of SEM-EDS performed in the FX-C xerogel and presented in EDS Analysis section of the **Supplementary Material**, compared favorably with the derived EDXRF values for the Ca/Si ratio equal to 0.08.

It is well-known that the degree of the hydrophobicity of the materials increases with the surface roughness. AFM measurements were performed in order to provide the depth field and morphological analysis of FX-C surface (Figure 5). Pseudocolors were used to explain the surface, with more bright colors to correspond to the most elevated features of the image, while the darker represent the deepest ones. In particular, the patchy areas are exhibited with light yellow or brown color, depending on the dynamic range of the surface topography. The surface displays variation in the topography image, thus indicating remarkable roughness.

TABLE 2 | Correlation of the uptake and dry matter of the FX-C treated samples along with the porosity and average pore diameter of their untreated counterparts.

Treated samples	Uptake (g/cm^2) 10^{-3}	Dry matter (g/cm^2) 10^{-3}	Porosity* (%)	Average Pore* diameter (μm)
Sound	6.00 \pm 0.40	2.40 \pm 0.16	11.98	0.031
Non-standard	12.50 \pm 0.78	3.60 \pm 0.06	13.21	0.038
Freeze-thaw	25.91 \pm 1.85	12.44 \pm 5.67	14.55	0.063
Carbonation	3.14 \pm 1.26	1.26 \pm 0.49	10.00	0.037
Chloride attack	13.25 \pm 6.44	5.70 \pm 2.77	11.89	0.034

*Untreated samples.

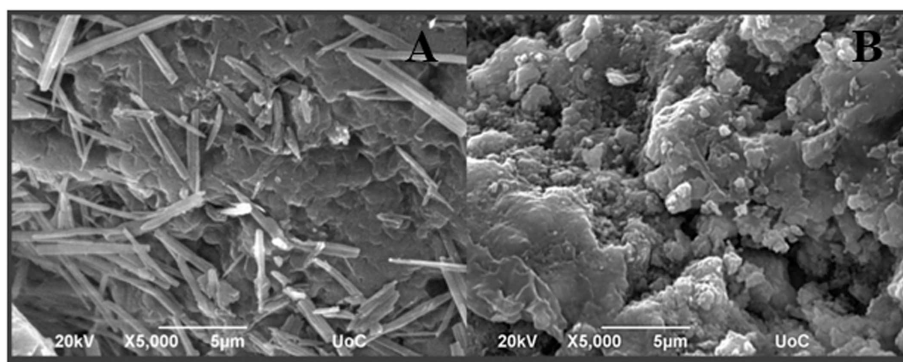


FIGURE 6 | SEM micrographs of (A) untreated freeze-thaw cement mortars and (B) freeze-thaw cement mortars treated with FX-C.

The reference plane divides the whole image area vertically, into two equal parts. The AFM image of FX-C shows a highly heterogeneous surface with patchy areas. The arithmetic mean of the roughness (R_a) and the square root (R_q) were estimated to 3.369 and 4.342 nm, respectively. These values of roughness are higher than the corresponding ones of traditional consolidants, showing a remarkable surface roughness, achieved by the described synthetic route (Petronella et al., 2018).

The Thermogravimetry/Differential Thermal Analysis (TG/DTA) curves of FX-C and synthesized CaOx nanoparticles (see **Figure S1**) show three endothermic peaks, which correspond to the thermal decomposition of CaOx.

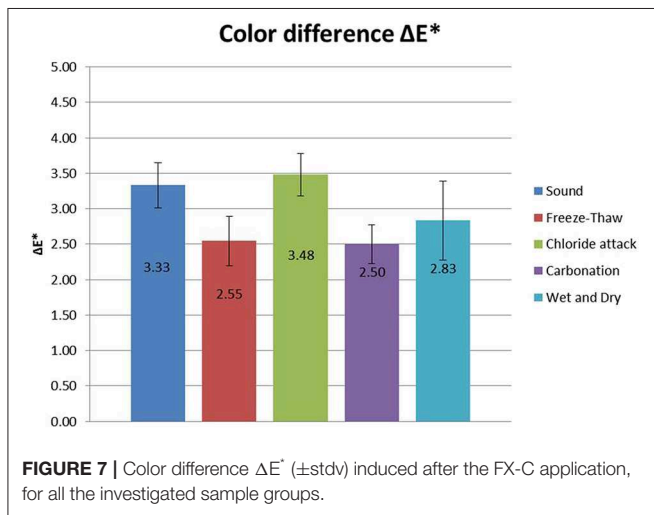


FIGURE 7 | Color difference ΔE^* (±stdv) induced after the FX-C application, for all the investigated sample groups.

Evaluation of the Consolidation Performance

The amount of the FX-C that was absorbed by the treated surfaces of sound and aged samples is presented in **Table 2**. Uptake varies according to the porosity of each investigated sample group. High amount of the consolidant was absorbed by the chloride attacked samples, non-standard and aged via freeze-thaw cycles, which is correlated with their higher total porosity and average pore size diameter. However, as we expected, the carbonated samples absorbed lower quantity than the sound mortars, due to their lower total porosity. Portlandite, as a consequence of the carbonation process, reacts with the CO_2 precipitating CaCO_3 , which in turn filled the pores and makes the sol penetration in the substrate difficult.

The different dry matter of the treated substrates is in direct relationship with the values of the open porosity as presented in **Table 2**.

Textural Properties

Figure 6 illustrates the SEM micrographs of freeze-thaw cement samples (**Figure 6A**) and their treated with FX-C counterparts (**Figure 6B**). The untreated cement sample exhibits cement hydration crystals in needle-like or rod-like shape. The needle-like crystals resemble ettringite crystals formed in aged cement samples under sulfate attack. However, as it can be clearly seen, the treated sample is characterized by the absence of needle-like crystals and deposition of FX-C on the CSH phases, concentrated at the boundaries of grains without blocking the pores, thus contributing to the enhancement of the consolidation efficiency. The extended network of FX-C displays a remarkable coverage capability of cement rods. It seems that between the CSH of cement and the modified-TEOS with CaOx and PDMS a network was formed giving rise to a denser microstructure which binds the grains more firmly.

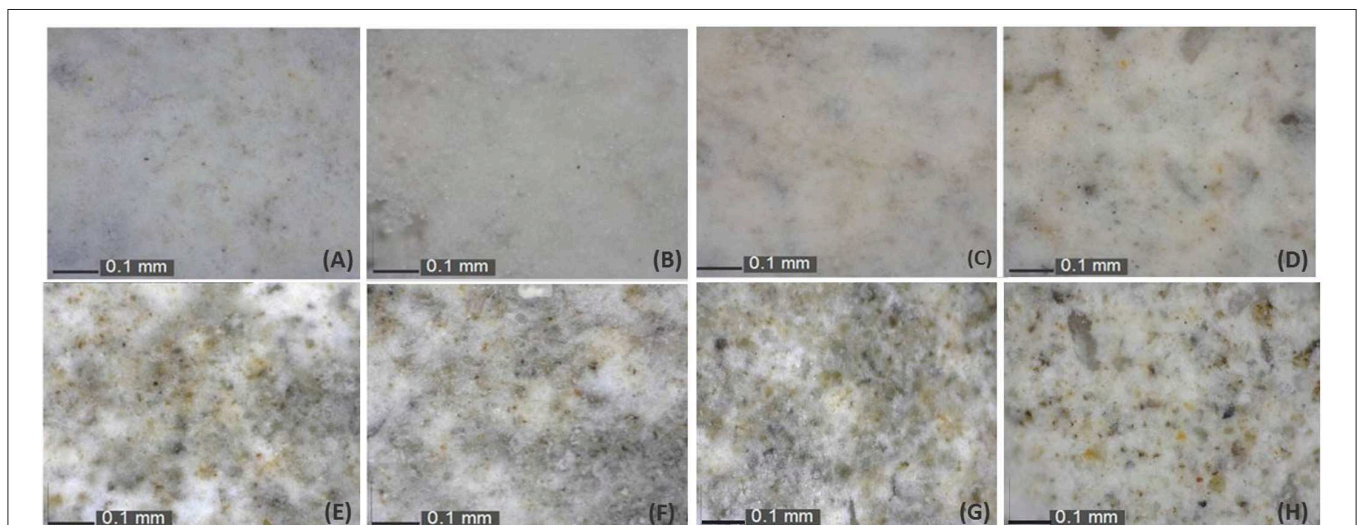


FIGURE 8 | Optical microscope images captured before (A,C,E,G) and after (B,D,F,H) samples treatment with FX-C for: sound (A,B), freeze-thaw (C,D), carbonated (E,F), and chloride-attacked (G,H) aged mortars.

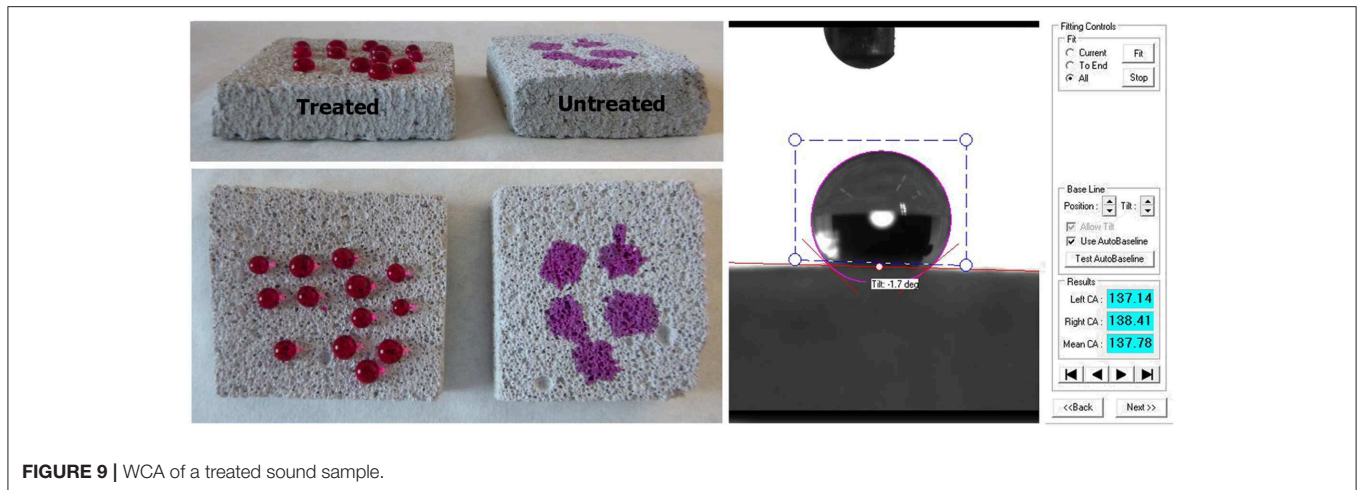


FIGURE 9 | WCA of a treated sound sample.

Aesthetic Parameters

The color changes induced after the FX-C application at the mortar surfaces were measured and are expressed as variations of ΔE^* (Figure 7). Taking into account that the general accepted threshold value for ΔE^* is equal to 5 (De Rosario et al., 2015; Ksinopoulou et al., 2016), the obtained values for the treated samples, are lower than the accepted limit.

The results of the application of the consolidant revealed that for the freeze-thaw and carbonated samples, the color change induced was insignificant. Although, sound and chloride attacked samples slightly surpassed this level, they still remained under the commonly accepted threshold for ΔE^* (equal to 5) (Figure 7).

The optical microscopy images of treated samples with FX-C are illustrated in Figure 8. The treated samples seem to be aesthetically similar to their untreated counterparts, having almost no alterations onto their surfaces. The magnified images reveal no cracking at the treated surfaces that is probably attributed to the PDMS low surface energy and the consequent prevention of TEOS cracking.

Water Repellency

Water Contact Angle (WCA) tests on sound cement samples presented in Figure 9, revealed that FX-C created a hydrophobic layer on the surface. WCA measurements were carried out in all of the sample groups treated with FX-C, and the corresponding bar diagram is presented in Figure S5. The WCA values of the treated samples ranged from 90 to 100 ($^\circ$) exhibiting a considerable increase comparing to their untreated counterparts (Figure S5).

Water repellency also seems to be successfully improved, as assessed by the capillary absorption test. More specifically, the water absorption by capillary coefficient (WAC) illustrated in Table 3 has significantly decreased especially in the aged samples, proving that FX-C penetrated into the pore system of the substrate, thus protecting against the action of water.

Mechanical Properties

The improvement of the mechanical behavior of the samples was studied in a non-destructive way by measuring the ultrasound

TABLE 3 | Water absorption by capillarity (WAC) coefficient of untreated and treated sound and aged samples measured in $\text{kg/m}^2 \cdot \text{s}^{1/2}$.

Set	Untreated ($\times 10^{-3}$)	Treated ($\times 10^{-3}$)	% Reduction of coefficient
Sound	18.6 \pm 1.1	17.9 \pm 0.6	3.76
Chloride attack	25.0 \pm 5.0	15.2 \pm 2.7	39.30
Freeze thaw	34.8 \pm 2.3	30.0 \pm 5.2	13.79
Carbonated	5.5 \pm 1.0	4.4 \pm 0.7	20.00

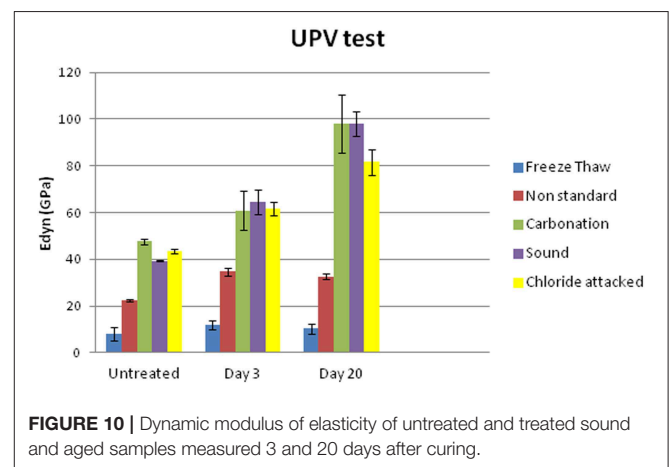


FIGURE 10 | Dynamic modulus of elasticity of untreated and treated sound and aged samples measured 3 and 20 days after curing.

pulse velocity (UPV), so that it could be inspected in a comparable procedure on site. Dynamic modulus of elasticity (E_{dyn}) has increased after the treatment for all sample sets of aging as illustrated in Figure 10, proving that FX-C achieved to re-aggregate the mortar microstructure.

Comparing the results of UPV test with the uptake of the product previously shown in Table 2, it is remarkable that freeze thaw aged samples, despite the high uptake of FX-C,

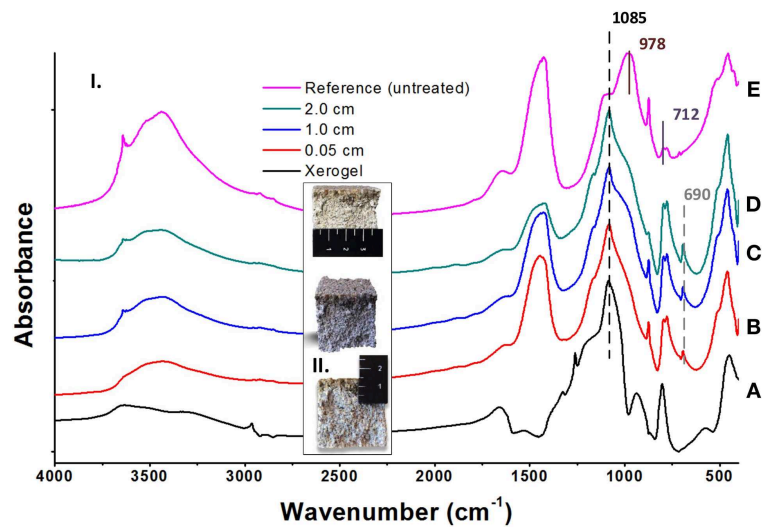


FIGURE 11 | Estimation of the FX-C penetration depth: (I) FTIR spectra of pure xerogel (A), cross-sections of treated depth from the surface (B: 0.05 cm, C: 1.0 cm, and D: 2.0 cm) and untreated (E) OPC mortar specimens; (II) Images of the cross-sections showing the penetration depth of the consolidant.

maintained the lowest values of E_{dyn} even after treatment. This could be explained by the high open porosity of samples indicated by the WAC coefficients shown in **Table 3**. Untreated samples from freeze thaw set exhibited the highest WAC coefficient, equal to $34.8 \pm 2.3 \text{ kg/m}^2 \cdot \text{s}^{1/2}$, which was reduced by 13.79% after treatment, thus maintaining a pore system that partially filled with consolidant, therefore, this was also reflected to the lowest E_{dyn} values comparing with the other samples.

Adhesion of the Treatment

Peeling test revealed almost insignificant removal of the FX-C for all the treated sample groups. This means that a good cohesion with the substrate was achieved, as no retained quantity was found onto the scotch tape after treatment. More specifically, concerning the treated, freeze-thaw and non-standard mortars an important reduction of the removal substrate was observed. The good adhesion of treatment to the mortar surface involved improvement of mechanical properties and water repellency.

Penetration Depth

In order to evaluate the penetration depth of the consolidant, FTIR spectra were collected before and after treatment of a non-standard sample. In particular, powders originating from the surface layer of the untreated sample and from different depths from the surface of a cross section of the same treated sample were examined (see **Figure 11**). These spectra were compared with the spectrum of the FX-C xerogel. The appearance of the xerogel characteristic peak at $1,085 \text{ cm}^{-1}$ owed to the Si-O-Si formation, was considered indicative of the consolidant presence. Consequently, the penetration depth of the FX-C seems to be more than 2 cm, after the consolidation process (spectrum D of the **Figure 11**). This is a significant indication of the FX-C penetration depth and the successful treatment of the

mortars. Deconvolution process of the above spectra is included in **Supplementary Material** evidencing that the band at $1,085 \text{ cm}^{-1}$ refers to the Si-O-Si of the xerogel and does not appear to the untreated sample.

CONCLUSIONS

A monolithic, non-toxic hydrophobic consolidant, namely FX-C, has been developed in an eco-friendly, one-pot procedure, incorporating to TEOS, PDMS, and nano calcium oxalate. CaOx displays a key role, due to its chemical affinity with the carbonate fragments which exist as aggregates in the concrete. Furthermore, FX-C, due to silica network and CaOx exhibited significant affinity to both siliceous and carbonate nature substrates, such as concrete and cement mortars. The derived product penetrated at least 2 cm into the cement mortar substrate affecting positively its mechanical properties, such as dynamic modulus of elasticity. Water repellency of the treated samples was particularly improved as indicated from WCA measurements and water absorption tests by capillarity. Absorption coefficients decreased 3–75% for sound and aged samples, respectively, and WCA was more than 90° at the treated samples. The treatment didn't alter the color of the surfaces and adhered well, as proved by the peeling test. Finally the absence of harmful byproducts after treatment established FX-C as a powerful consolidant for strengthening and protecting concrete structures.

DATA AVAILABILITY STATEMENT

All datasets generated for this study are included in the article/**Supplementary Material**.

AUTHOR CONTRIBUTIONS

KK, EV, and DS designed, performed the experiments, analyzed the experimental data, and collaborated in the writing of the paper. AF, GA, and IA carried out the experiments. IG-L and MB-V manufactured the OPC samples, carried out experiments, and reviewed the paper. PM conceived and designed the research, supervised the research activities, analyzed the experimental data, and wrote the paper.

FUNDING

This work has been supported by the InnovaConcrete project funded by the European program Horizon 2020 (GA no. 760858).

REFERENCES

- Baglioni, P., Chelazzi, D., Giorgi, R., and Poggi, G. (2013). Colloid and materials science for the conservation of cultural heritage: cleaning, consolidation and deacidification. *Langmuir* 29, 5110–5122. doi: 10.1021/la304456n
- Barberena-Fernández, A. M., Blanco-Varela, M. T., and Carmona-Quiroga, P. M. (2018). Use of nanosilica- or nanolime-added TEOS to consolidate cementitious materials in heritage structures: physical and mechanical properties of mortars. *Cement Concrete Composites* 95, 42–55. doi: 10.1016/j.cemconcomp.2018.09.011
- Barberena-Fernández, A. M., Carmona-Quiroga, P. M., and Blanco-Varela, M. T. (2015). Interaction of TEOS with cementitious materials: chemical and physical effects. *Cement Concrete Composites* 55, 145–152. doi: 10.1016/j.cemconcomp.2014.09.010
- Berry, J. D., Neeson, M. J., Dagastine, R. R., Chan, D. Y. C., and Tabor, R. F. (2015). Measurement of surface and interfacial tension using pendant drop tensiometry. *J. Colloid Interface Sci.* 454, 226–237. doi: 10.1016/j.jcis.2015.05.012
- De Rosario, I., Elhaddad, F., Pan, A., Benavides, R., Rivas, T., and Mosquera, M. J. (2015). Effectiveness of a novel consolidant on granite: laboratory and *in situ* results. *Constr. Build. Mater.* 76, 140–149. doi: 10.1016/j.conbuildmat.2014.11.055
- Facio, D. S., Carrascosa, L. A. M., and Mosquera, M. J. (2017). Producing lasting amphiphobic building surfaces with self-cleaning properties. *Nanotechnology* 28:265601. doi: 10.1088/1361-6528/aa73a3
- Franzoni, E., Graziani, G., Sassoni, E., Bacilieri, G., Griffa, M., and Lura, P. (2014). Solvent-based ethyl silicate for stone consolidation: influence of the application technique on penetration depth, efficacy and pore occlusion. *Mater. Struct.* 48, 3503–3515. doi: 10.1617/s11527-014-0417-1
- Illescas, J. F., and Mosquera, M. J. (2012). Producing surfactant-synthesized nanomaterials *in situ* on a building substrate, without volatile organic compounds. *ACS Appl. Mater. Interfaces* 4, 4259–4269. doi: 10.1021/am300964q
- Ion, R. M., Teodorescu, S., Stirbescu, R. M., Bucurică, I. A., Dulamă, I. D., and Ion, M. L. (2017). Calcium oxalate on limestone surface of heritage buildings. *Key Eng. Mater.* 750, 129–134. doi: 10.4028/www.scientific.net/KEM.750.129
- Kapridaki, C., and Maravelaki-Kalaitzaki, P. (2013). TiO₂-SiO₂-PDMS nano-composite hydrophobic coating with self-cleaning properties for marble protection. *Prog. Org. Coatings* 76, 400–410. doi: 10.1016/j.porgcoat.2012.10.006
- Karapanagiotis, I., Pavlou, A., Manoudis, P. N., and Aifantis, K. E. (2014). Water repellent ORMOSIL films for the protection of stone and other materials. *Mater. Lett.* 131, 276–279. doi: 10.1016/j.matlet.2014.05.163
- Ksinopoulou, E., Bakolas, A., and Moropoulou, A. (2016). Modifying Si-based consolidants through the addition of colloidal nano-particles. *Appl. Phys. A* 122:267. doi: 10.1007/s00339-016-9772-9

ACKNOWLEDGMENTS

The authors are also grateful for the technical and scientific support part of this research to the: University of Crete, Microscope lab of the Biology Department (Stefanos Papadakis) and Microelectronics Research Group (Aikaterini Tsagaraki), MIRTEC (Dr. Dia Andreouli) and TUC (Prof. Chrysikopoulos and Theodosia Fountouli, Prof. N. Passadakis, E. Chamilaki, Dr. A. Stratakis, and S. Mavriannakis).

SUPPLEMENTARY MATERIAL

The Supplementary Material for this article can be found online at: <https://www.frontiersin.org/articles/10.3389/fmats.2020.00016/full#supplementary-material>

- Lin, M.-H., Song, Y.-L., Lo, P.-A., Hsu, C.-Y., Lin, A. T. L., Huang, E. Y.-H., et al. (2019). Quantitative analysis of calcium oxalate hydrate urinary stones using FTIR and 950/912 cm⁻¹ peak ratio. *Vibrational Spectrosc.* 102, 85–90. doi: 10.1016/j.vibspec.2019.03.006
- Lollino, G., Giordan, D., Marunteanu, C., Christaras, B., Yoshinori, I., and Margottini, C. (2015). *Engineering Geology for Society and Territory – Volume 8*. Cham: Springer International Publishing.
- Maravelaki, N., Verganelaki, A., Kilikoglou, V., and Karatasios, I. (2014). Synthesis and characterization of a calcium oxalate-silica nanocomposite for stone conservation. *Eng. Geol. Soc. Territory* 8, 525–529. doi: 10.1007/978-3-319-09408-3_93
- Maravelaki-Kalaitzaki, P., Kallithrakas-Kontos, N., Korakaki, D., Agioutantis, Z., and Maurigiannakis, S. (2006). Evaluation of silicon-based strengthening agents on porous limestones. *Prog. Org. Coat.* 57, 140–148. doi: 10.1016/j.porgcoat.2006.08.007
- Miliani, C., Velo-Simpson, M. L., and Scherer, G. W. (2007). Particle-modified consolidants: a study on the effect of particles on sol-gel properties and consolidation effectiveness. *J. Cult. Herit.* 8, 1–6. doi: 10.1016/j.culher.2006.10.002
- Moropoulou, A., Cakmak, A., Labropoulos, K. C., Van Grieken, R., and Torfs, K. (2004). Accelerated microstructural evolution of a calcium-silicate-hydrate (C-S-H) phase in pozzolanic pastes using fine siliceous sources: comparison with historic pozzolanic mortars. *Cement Concrete Res.* 34, 1–6. doi: 10.1016/S0008-8846(03)00187-X
- Mosquera, M. J., de los Santos, D. M., and Rivas, T. (2010). Surfactant-synthesized ormosils with application to stone restoration. *Langmuir* 26, 6737–6745. doi: 10.1021/la9040979
- Pan, X., Shi, Z., Shi, C., Ling, T.-C., and Li, N. (2017). A review on surface treatment for concrete – part 2: performance. *Constr. Build. Mater.* 133, 81–90. doi: 10.1016/j.conbuildmat.2016.11.128
- Petronella, F., Pagliarulo, A., Truppi, A., Lettieri, M., Masieri, M., Calia, A., et al. (2018). TiO₂ nanocrystal based coatings for the protection of architectural stone: the effect of solvents in the spray-coating application for a self-cleaning surfaces. *Coatings* 8:356. doi: 10.3390/coatings8100356
- Pigino, B., Leemann, A., Franzoni, E., and Lura, P. (2012). Ethyl silicate for surface treatment of concrete – part II: characteristics and performance. *Cement Concrete Composites* 34, 313–321. doi: 10.1016/j.cemconcomp.2011.11.021
- Pinho, L., Elhaddad, F., Facio, D. S., and Mosquera, M. J. (2013). A novel TiO₂-SiO₂ nanocomposite converts a very friable stone into a self-cleaning building material. *Appl. Surface Sci.* 275, 389–396. doi: 10.1016/j.apsusc.2012.10.142
- Rodriguez-Navarro, C., Suzuki, A., and Ruiz-Agudo, E. (2013). Alcohol dispersions of calcium hydroxide nanoparticles for stone conservation. *Langmuir*, 29, 11457–11470. doi: 10.1021/la4017728

- Ruffolo, S. A., and La Russa, M. F. (2019). Nanostructured coatings for stone protection: an overview. *Front. Mater.* 6:147. doi: 10.3389/fmats.2019.00147
- Sandrolini, F., Franzoni, E., and Pignino, B. (2012). Ethyl silicate for surface treatment of concrete – part I: pozzolanic effect of ethyl silicate. *Cement Concrete Composites* 34, 306–312. doi: 10.1016/j.cemconcomp.2011.12.003
- Scherer, G. W., and Wheeler, G. S. (2009). Silicate consolidants for stone. *Key Eng. Mater.* 391, 1–25. doi: 10.4028/www.scientific.net/KEM.391.1
- Schutter, G.D. (2012). *Damages to Concrete Structures*, Boca Raton, FL; London; New York, NY: CRC Press, Taylor & Francis Group.
- Son, S., Won, J., Kim, J. J., Jang, Y. D., Kang, Y. S., and Kim, S. D. (2009). Organic-Inorganic hybrid compounds containing polyhedral oligomeric silsesquioxane for conservation of stone heritage. *ACS Appl. Mater. Interfaces* 1, 393–401. doi: 10.1021/am800105t
- Verganelaki, A., Kapridaki, C., and Maravelaki-Kalaitzaki, P. (2015). Modified tetraethoxysilane with nanocalcium oxalate in one-pot synthesis for protection of building materials. *Ind. Eng. Chem. Res.* 54, 7195–7206. doi: 10.1021/acs.iecr.5b00247
- Verganelaki, A., Kilikoglou, V., Karatasios, I., and Maravelaki-Kalaitzaki, P. (2014). A biomimetic approach to strengthen and protect construction materials with a novel calcium-oxalate–silica nanocomposite. *Constr. Build. Mater.* 62, 8–17. doi: 10.1016/j.conbuildmat.2014.01.079

Conflict of Interest: GA and IA were employed by the company 'NanoPhos S.A.'.

The remaining authors declare that the research was conducted in the absence of any commercial or financial relationships that could be construed as a potential conflict of interest.

Copyright © 2020 Kapetanaki, Vazgiouraki, Stefanakis, Fotiou, Anyfantis, García-Lodeiro, Blanco-Varela, Arabatzis and Maravelaki. This is an open-access article distributed under the terms of the Creative Commons Attribution License (CC BY). The use, distribution or reproduction in other forums is permitted, provided the original author(s) and the copyright owner(s) are credited and that the original publication in this journal is cited, in accordance with accepted academic practice. No use, distribution or reproduction is permitted which does not comply with these terms.